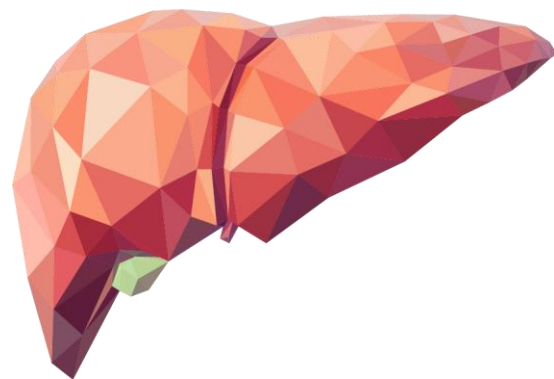


MASTER THESIS

Image-guided liver interventions: Ablation assessment and MR-guided liver biopsy



Tom Perik, BSc

TECHNICAL MEDICINE

EXAMINATION COMMITTEE

Prof. dr. J.J. Fütterer

Dr. K. Overduin

Dr. ir. F.F.J. Simonis

Dr. M. Groenier

Prof. dr. ir. R.M. Verdaasdonk

UNIVERSITY OF TWENTE.

Radboudumc

Preface

Before you lies my thesis which was written in order to obtain the Master of Science degree in Technical Medicine, with a specialization in Medical Imaging and Interventions, at the University of Twente. It presents the research conducted at the department of Radiology and Nuclear Medicine of the Radboudumc in Nijmegen during the clinical specialization internship.

Several persons have contributed to the realization of this thesis whom therefore deserve acknowledgement. First of all, I would like to express my gratitude to Jurgen, Kristian, Frank, and Marleen for their medical, technical, and process supervision. I would like to thank my colleagues of the MAGIC research group for their scientific support and mental support during this year. Furthermore, I thank my fellow clinical technologist, Ilse, Ilse and Thomas for sharing experiences during intervention.

Finally, I would like to thank my family, friends, my sister Ilse, and Emma for their support and for always showing genuine interest.

Table of contents

Preface.....	3
Chapter 1. Introduction.....	7
Chapter 2. Retrospective analysis of 3D ablation zones after thermal ablation of liver tumors.....	9
Introduction.....	9
Materials and methods	9
Results	13
Discussion	16
.....	18
Chapter 3. Workflow for MR-guided liver biopsy for liver lesions in patients with pancreatic cancer	20
Introduction.....	20
Materials & Methods	21
Discussion	24
Conclusion	27
Chapter 4: META-PANC study, first clinical experience	29
Introduction.....	29
Materials & Methods	29
Case examples	29
Discussion	32
Chapter 5: Conclusions & Future perspective.....	33
Future Perspectives.....	33
References.....	35
Appendix A: Diffusion-weighted imaging.....	39

Chapter 1. Introduction

General introduction

Interventional radiology is a medical specialization which utilizes minimally-invasive image-guided procedures to diagnose and treat diseases in nearly every organ system. These procedures have shown to result in fewer complications, faster recoveries and therefore reduced costs.¹ A subfield of interventional radiology is interventional oncology which uses interventional techniques for the diagnosis and treatment of cancers, with applications in several fields such as prostate cancer and kidney cancer. Interventional oncology is also increasingly used for diagnostic and therapeutic procedures in the liver. Interventional treatments in the liver include percutaneous ablation, transarterial chemoembolization (TACE) and internal radiation therapy. For treatment of liver tumors, thermal ablation therapy has developed as a minimally invasive local treatment with curative potential. This local treatment is used for both primary liver tumors, such as hepatocellular carcinoma (HCC) and secondary tumors, mainly colorectal liver metastases (CRLM). During percutaneous thermal ablation, probes are inserted into the tumor using image guidance and thermal energy is applied to eradicate the tumor. This can be in the form of radiofrequency ablation (RFA) using alternating radiofrequency currents (375-480 kHz) or microwave ablation (MWA) using electromagnetic waves (300 MHz-300 GHz). When compared to surgery, percutaneous ablation shows lower complication rates and serves as a viable alternative.² However treatment efficacy is impeded by local tumor recurrence, with reported rates up to 31%.³

For diagnosis, liver biopsies are performed to acquire hepatic tissue for histopathological assessment to determine the cause of liver disease or focal liver lesions. In clinical practice most lesions are diagnosed using contrast-enhanced CT or MRI imaging alone. But histopathological confirmation is useful when imaging is inconclusive or confirmation is necessary for research purposes. Currently biopsies are performed using ultrasound-guidance as this is a fast and cheap procedure.

Motivation for study

In the Radboudumc percutaneous thermal liver ablation is performed since several years. The clinical effectiveness in terms of local tumor control of all these treatments in this centre is never assessed before. The necessary treatment margin necessary to prevent local tumor progression is still debated in literature. The current treatment assessment is performed by visually comparing two-dimensional pre-ablation imaging (CT or MRI) with post-ablation imaging (CT). This comparison is often impeded by misalignment of the liver, due breathing motion or liver deformation. With visualization software a three-dimensional treatment assessment can be performed by registration of pre- and post-ablation images. Retrospective three-dimensional ablation assessment could help in the assessment of ablation zone margins and possibly help the prediction of treatment outcome.

In the Radboudumc the DIA-PANC study is running, which uses diffusion-weighted MRI (DWI) for the detection of liver metastases in patients with pancreatic cancer. These liver lesions are very small and often only visible on diffusion-weighted MRI (DWI), using current imaging guidance used for biopsy (ultrasound or CT) these lesions cannot be biopsied. MRI-guidance might be a possible option for biopsy of these liver lesions.

Main aim of this thesis

The main goal is to improve image guidance of liver interventions by focusing on both the treatment assessment after liver ablation and MR-guidance during liver biopsy. For thermal ablation treatment

assessment could be improved using three-dimensional (3D) visualization software. A retrospective study was performed to analyse ablation margins and assess the local recurrence rate in the Radboudumc. To improve targeting of liver biopsy in patients with pancreatic cancer we developed a workflow for MRI-guided biopsy, this workflow was tested. The clinical application of the workflow will be tested in a clinical study.

The following research questions were formulated:

Ablation assessment

- What is the local recurrence rate after percutaneous thermal ablation in the Radboudumc?
- Can three-dimensional visualization software help to predict local tumor progression after ablation?
 - o Is there a correlation between three-dimensional ablation margins and local tumor recurrence?
 - o What is an advisable minimal ablation margin to prevent local tumor recurrence?

MR-guided biopsy

- Is it feasible to perform MR-guided biopsy of suspected liver lesions in patients with pancreatic cancer?
 - o Can an adequate clinical workflow for MR-guided liver biopsy be developed?
 - o Can this technique safely be implemented in patients?

Thesis outline

A general introduction to the topic of interventional radiology and image guidance was provided and the main objectives were formulated. (Chapter 1)

A retrospective analysis of ablation zones after thermal ablation of liver tumors was performed. In this study images before and after the ablation were registered to assess the reached ablation margins, these margins were correlated with clinical outcome of the patients. (Chapter 2)

A workflow for MR-guided biopsy for possible liver metastases in patients with pancreatic cancer was designed. The design steps and considerations for the imaging protocol and workflow are described. (Chapter 3)

The first two MR-guided biopsies were performed, these clinical cases are described and evaluated. (Chapter 4)

The final chapter describes the general outcomes and provides a main conclusion. Furthermore future recommendations for research and clinical practice are described. (Chapter 5)

Chapter 2. Retrospective analysis of 3D ablation zones after thermal ablation of liver tumors

Introduction

Percutaneous image-guided thermal ablations of the liver have evolved into a widely used therapeutic treatment for primary and secondary hepatic malignancies. The most widely used form of ablation therapy is thermal ablation including therapies such as radiofrequency ablation (RFA) and microwave ablation (MWA). Both these methods create zones of coagulative necrosis through the application of heat to eradicate the tumor tissue. When a temperature above 60°C is reached, this will almost immediately lead to irreversible damage in the cells.⁴ This focal therapy has proven to be a relative low-risk procedure for the treatment of focal liver tumors.^{5,6} Advantages of percutaneous ablation are a shorter hospitalisation and a low morbidity and mortality rate.² However, local tumor progression (LTP), defined as the appearance of new tumor area at the ablative margin after local ablation treatment is a major drawback of this therapy, with reported local tumor progression rates of 8-31%.^{3,7-10} There are several known risk factors for local tumor progression including large tumor size (>3 cm), blood vessels in vicinity of tumor and insufficient ablation margins.^{11,12,13} With larger tumor size, the likelihood of local tumor progression increases as a result of satellite nodules¹⁴, therefore several studies advise a minimal margin of 5 mm around the tumor.^{12,15,13,16}

As LTP is a direct consequence of insufficient ablation margins, sufficient ablation margins can lower the local recurrence rate and prevent the need for additional therapy. Therefore the ablation margin is recognised as an important parameter of the ablation efficacy and predictor of local recurrence. Currently, margin assessment after thermal ablation is performed by estimating the distance between radiographic boundaries of the tumor and the ablation zone using visual comparison of pre- and post-ablation in two dimensional images. This approach is hindered by misalignment of the liver between pre-ablation scans and post-ablation scans due to breathing motion, liver deformation and heating-induced tissue changes. The second disadvantage is that the minimal margin does not indicate the extent of tissue that does not reach the minimal margin, which determines the tissue that needs additional ablation to ensure adequate margins. A 3D quantitative assessment can overcome these limitations and provide a more accurate evaluation of ablation zone margins. Several studies show the feasibility of 3D assessment of ablation zones in the liver and the potential to detect undertreated tumors.^{13,17,18} Intraoperative assessment of ablation margins could improve treatment accuracy and potentially reduce the local tumor progression and recurrence rates.^{12,19}

The purpose of this study is to retrospectively determine the clinical outcomes and assess the 3D ablation margins achieved in thermal ablation of liver tumors.

Materials and methods

Patient population

Patients were included who underwent a thermal ablation therapy of a liver tumor at the Radboudumc (Nijmegen, the Netherlands) between 1 January 2016 and 31 May 2019. To be eligible for analysis patients had to have pre- and post-ablation imaging available and at least one follow-up scan. A total of 58 patients (median age 58, range 25-83, males/females=35/23) met the inclusion criteria and were included for this retrospective analysis. In these patients a total of 74 tumors was treated. The liver tumors were diagnosed based on radiologic features using contrast-enhanced CT imaging (n=34) or

dynamic contrast-enhanced MR imaging (n=24). The tumor type distribution was as follows 27 HCC, 27 CRLM and 4 other liver tumors (FNH, haemangioma endothelium, mamma carcinoma metastasis and a neuroendocrine tumor). Twenty-five patients had liver cirrhosis, all in the HCC group, classified according to the Child-Pugh score 22 patients in class A, 2 in class B and 1 in class C. For 30 patients, ablation was the first treatment in the liver, while 28 patients underwent prior treatment (TACE (n=9), partial liver resection (n=9), chemotherapy (n=7), irreversible electroporation (IRE) (n=3)). The decision to perform thermal ablation was made by the multidisciplinary tumor board. A summary of patient demographic data is provided in Table 1.

Table 1: Patient demographic data, general information of all included patients. Second part of the table contains general information about the tumors included into the LTP analysis.

Patient information (n=58)	n (%) or Median (range)
Gender	
<i>Male</i>	35 (60%)
<i>Female</i>	23 (40%)
Age	58 (range: 25-83)
Liver cirrhosis	
<i>Yes</i>	25 (43%)
<i>No</i>	33 (57%)
Prior treatment	
<i>None</i>	30 (51%)
<i>Chemotherapy</i>	7 (12%)
<i>TACE</i>	9 (16%)
<i>Partial liver resection</i>	9 (16%)
<i>IRE</i>	3 (5%)
Tumor type	
<i>HCC</i>	27 (46%)
<i>CRLM</i>	27 (46%)
<i>Miscellaneous</i>	4 (8%)
Lesion information (n=74)	n (%) or Median (range)
Location	
<i>Subcapsular (< 1cm of border)</i>	38 (50%)
<i>Non-subcapsular</i>	38 (50%)
Lesion size (mm)	2.0 (range: 0.5-43)
Lesion volume (ml)	1.9 (range: 0.2-40)
Vessel within 1 cm	
<i>Yes</i>	18 (24%)
<i>No</i>	56 (76%)

Pre-ablation imaging

Prior to the ablation procedure, all patients underwent CT and/or MR imaging as part of routine staging work-up. Pre-ablation CT imaging was performed on a single CT-scanner (Toshiba Aquilion One) using a four phase liver protocol that included blanco and arterial, portal-venous and late contrast-enhanced imaging. Pre-ablation MR imaging was also performed on a single MR scanner (Skyra 3T, Siemens, Erlangen, Germany) using routine T2-w, DWI and contrast-enhanced imaging. For pre-ablation imaging MRI was used for 24 patients and CT for 34 patients. For MRI in 19 patients T1 viba contrast-enhanced

(3mm slice thickness) (venous (n=5), arterial (n=14)) was used and for 5 patients T2 HASTE (5mm slice thickness). For CT imaging arterial phase (n=16), portal venous phase (n=17), blanco (n=1).

Ablation procedures

All ablation procedures were performed by three experienced interventional radiologist and performed under general anaesthesia. 17 patients were treated with both RFA ablations and 41 patients with MWA. For RFA procedures a 14 gauge electrode (length in 10, 15 or 25 cm) (Starburst XL Electrode, RITA Medical systems) was used in combination with a 460 kHz generator (Model 1500X RF Generator, RITA Medical systems). For MWA procedures two systems were in use, the first is a 2.45 GHz generator with a maximum output of 100W with an internal water cooling (Emprint, Covidien Medtronic). The second MWA system is a 2.45 GHz with a maximum output of 195W and a CO₂-cooled system (Neuwave Ethicon, Johnson & Johnson Medical Devices), this system has the possibility of simultaneous multiprobe ablations for larger ablation zones. All ablation were performed in CT suite using the CT scanner (Toshiba Aquilion One) for post-ablation imaging.

The needle placement was performed under CT guidance (n=40) or ultrasound guidance (n=18) depending on the lesion location and lesion visibility. When the needle was placed correctly according to the interventional radiologist the ablation was started. Ablation power and duration of the ablation are determined on the basis of the size of the tumor.

After ablation, in all cases contrast-enhanced CT imaging was performed to assess the ablation zone in all cases. The used CT imaging had a slice thickness of 1 mm. All post-ablation scans were CT images performed on the same CT scanner (Acquilion ONE, Toshiba, Tokyo, Japan). These CT images were used to make a visually compared with preprocedural imaging to determine the overlap of ablation zone with the tumor in two dimensions. When tumor ablation was completed, track ablation was performed along the needle path to prevent possible tumor seeding. All patients remained under observation for treatment related complications and were generally discharged the day after the procedure. Mean follow-up time was 10 months (range: 1-24 months).

Table 2: Procedure characteristics, this table shows general information about the ablation procedures all information is divided by the number of patients (n=58)

Procedure information (n=58)	n (%)
Ablation type	
<i>MWA</i>	41 (71%)
<i>RFA</i>	17 (19%)
Image guidance	
<i>CT</i>	40 (74%)
<i>Ultrasound</i>	18 (26%)
Tumors treated during ablation procedure	
<i>1</i>	47 (81%)
<i>2</i>	10 (17%)
<i>3</i>	1 (2%)
Patients re-ablated	9 (16%)

Image analysis

All preprocedural and intraprocedural images were retrospectively reviewed using medical visualization software (Software Assistant for Needle Based Intervention, SAFIR, Fraunhofer MEVIS, Bremen, Germany). Preprocedural images were used to segment the boundaries of the treated tumors, both MRI and CT images are used for segmentation depending on availability of the imaging using a semi-automatic segmentation tool. The location of the tumor was defined manually with a marker, then the software segmented the tumor based on differences in contrast between the tumor and liver tissue. For the ablation zone, the same segmentation was performed in the post-ablation images (portal venous phase CT images). Based on anatomical landmarks in the liver, in particular liver vessels, the registration of pre- and post- ablation imaging was performed using a rigid manual registration in SAFIR. The registration accuracy and segmentation accuracy were checked by an experienced interventional radiologist. Maximal diameter of the tumor and corresponding ablation zone were derived from the segmentations. The ablation margins were calculated using a Hausdorff distance calculation. Hausdorff distance considers the mismatch between all possible relative positions of two sets (in this cases ablation zone and tumor), the minimal Hausdorff distance M_g is defined as:

$$M_G(A, B) = \min H(A, g B)$$

Volumes of undertreatment (margin <0mm), volume of minimal margin (margin 0-5 mm) and volume with a sufficient margin (margin >5 mm) were also calculated in the software.

For analysis of 3D ablation margins, successful registration and segmentation of both the tumor and ablation zone are necessary. Therefore, exclusion criteria were used to select eligible cases for 3D ablation margin assessment. The registration was visually scored following a three way scoring system: good, medium, poor. Registration was classified 'good' when the pre- and post-ablation was well aligned throughout the liver, 'medium' was given when local registration around the tumor location was accurate, but in the rest of the liver there was misaligned. Registration was labelled 'poor' when local registration had a misalignment of more than 5 mm (exact measurements were not possible in the software) in transversal view or a visible shift between transversal and coronal or sagittal view. Cases were excluded when visibility of the lesion or ablation zone was not sufficient for accurate segmentation cases and/or poor registration accuracy.

3D analysis

A case selection was performed before the 3D analysis, 13 tumors with a registration score 'Poor' were excluded for 3D margin analysis, as suboptimal registration impedes an accurate margin analysis. In tumors treated with TACE before ablation the ablation zone is difficult to delineate as TACE impedes the contrast enhancement which is necessary to delineate the ablation zone, therefore all tumors pre-treated with TACE were also excluded (n=10). In one case no post-ablation CT images were available and was therefore excluded. Tumors which were re-ablated after recurrence were also excluded (n=5). After exclusion 46 tumors were eligible for 3D analysis. The selection of eligible patients for the 3D analysis is shown in figure 1.

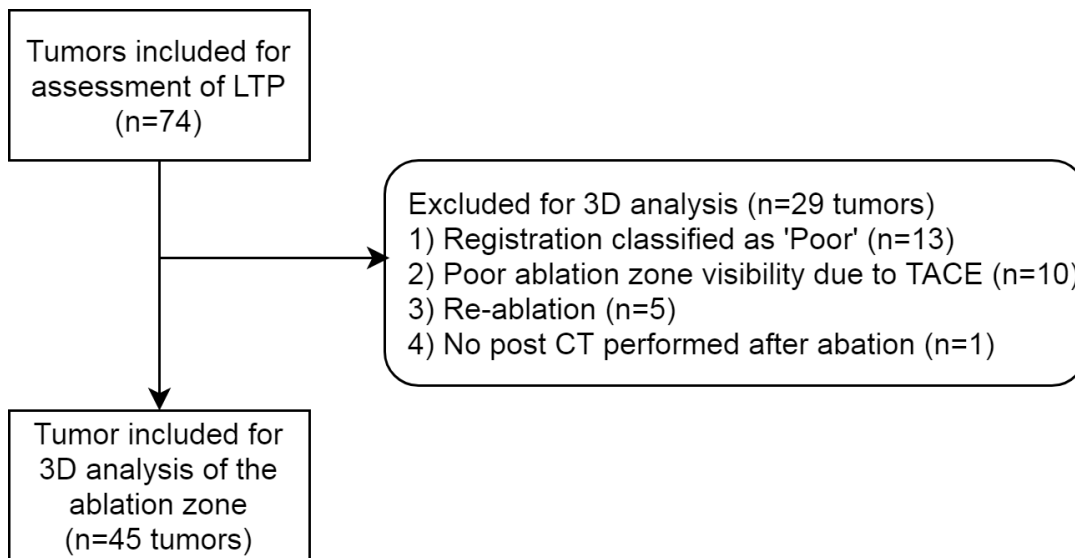


Figure 1: Flow diagram of the selection of tumor cases eligible for the 3D ablation zone analysis.

Statistical analysis

Statistics were performed using SPSS (version 25). Normal distribution was tested with Shapiro-Wilk test for comparative parameters of local tumor progression. Baseline parameters were compared between cases with local tumor progression and cases without local tumor progression using independent samples t-test for normally distributed data. For discrete data Chi-Square analysis was used. Survival analysis was performed using the Kaplan-Meier survival curves, log-rank test was used to assess differences between survival curves. P-values less than 0.05 were considered statistically significant.

Results

Local tumor progression

A total of 74 tumors were treated in 58 patients. Tumor types were distributed as follows 43 HCC, 27 CRLM and 4 miscellaneous type tumors. The median tumor volume was 1.9 ml (range 0.2-40.4 ml), and the median lesion size was 20 mm (range 5-43 mm). In 21 (28%) cases local tumor progression was found during follow-up. Distributed by tumor type HCC showed local tumor progression in 10/43(23%) tumors. CRLM showed local tumor progression in 8/27 (30%) tumors. The median time to local tumor progression was 6 months (range 1-24 months). Tumor volume was not statistically significant different between the group with and without local tumor progression ($p=0.280$). For lesion size no statistically significant difference was found between the two groups ($p=0.530$). There is also no statistical significant difference for the type of ablation, RFA or MWA ($p=0.917$). The distribution of baseline parameters between cases with local tumor progression and without local tumor progression can be found in table 3.

Table 3: The distribution of baseline parameters between the groups with local tumor progression and without local tumor progression is provided. No statistical significant difference between the groups was found for these parameters.

	Tumors with LTP n (% with LTP)	Tumors without LTP n (% without LTP)	p-value
Amount	21 (28%)	53 (72%)	
Tumor type			0.088
<i>HCC</i>	10 (23%)	33 (77%)	
<i>CRLM</i>	8 (30%)	19 (70%)	
<i>Miscellaneous</i>	3 (75%)	1 (25%)	
Location			0.439
<i>Subcapsular (<1 cm)</i>	12 (32%)	25 (67%)	
<i>Non-subcapsular</i>	9 (24%)	28 (76%)	
Median lesion size (mm)	2.1 (range: 1-3.3)	1.9 (range: 0.5-4.8)	0.530
Median tumor volume (ml)	2.4 (range: 0.2-18.0)	1.7 (range: 0.2-40)	0.280
Ablation type			0.917
<i>MWA</i>	14 (28%)	36 (72%)	
<i>RFA</i>	7 (29%)	17 (71%)	

3D Analysis

In the group included for 3D analysis (N=45), local tumor progression was found in 14 cases (31%) and local control in 31 cases (69%). The median minimal margin for the group with local tumor progression is -4.9mm (range: -1 to -20 mm). For the group with local control the median minimal margin was 0.8 mm (range: -5.6 to 6.2 mm). Figure 2 shows the distribution of the minimal ablation margin for cases with and without local tumor progression, the minimal margin is statistically significant smaller ($p=0.05$) in the local tumor progression group.

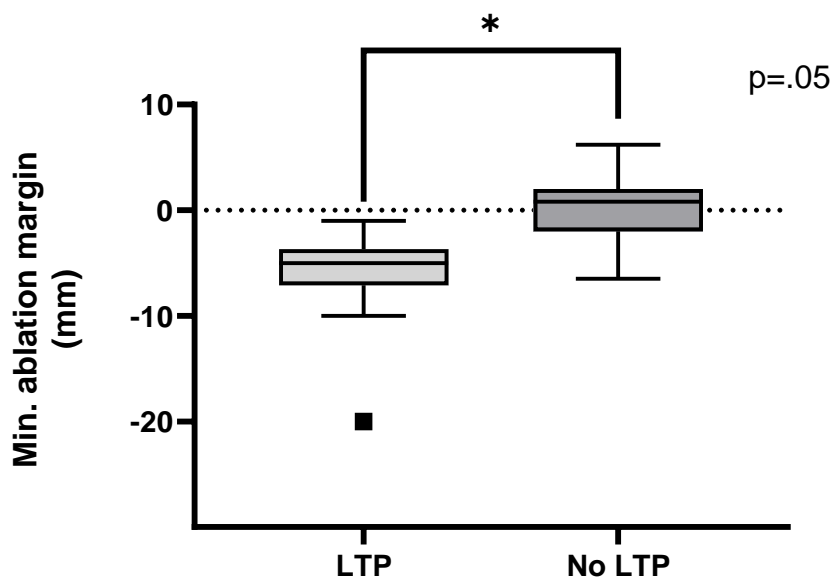


Figure 2: Minimal ablation margin split by local tumor progression (n=14) and the absence of local tumor progression (n=31). For the local tumor progression group all minimal ablation margins were negative. There is a significant difference between of minimal margins between both groups ($p=0.05$).

On Kaplan-Meier analysis, local tumor progression-free survival at 1 year after ablation is statistically improved between patients without negative margins (100%), margins between -5 and 0 mm (65%) and negative margins larger than 5mm (0%) ($p=0.001$) (Fig. 3). A log-rank test shows a significant difference between these groups of minimal margin ($p<0.001$). Kaplan-Meier analysis for the effect of percentage residual volume on the local tumor progression-free survival at 1 year between a group with no residual tumor (100%), with 0-20% residual tumor (63%) and the group with more than 20% residual tumor (0%) (Fig. 4). Log-rank test shows significant differences between these groups ($p=0.001$). Examples of the 3D analysis for tumor cases with and without local tumor progression are shown in figure 5 and figure 6.

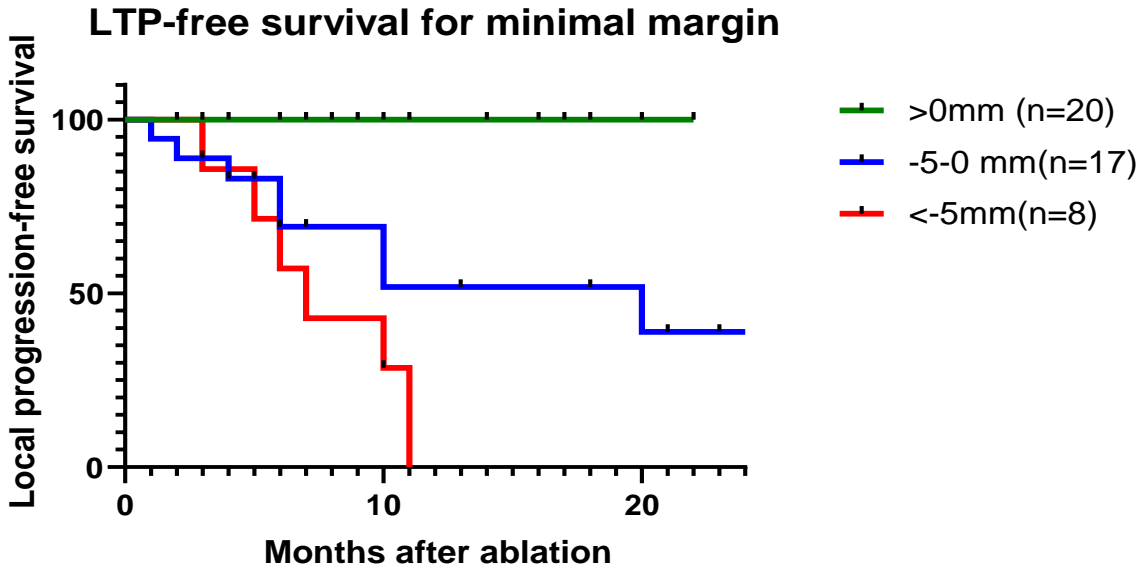


Figure 3: Kaplan-Meier curve for local progression-free survival stratified by the minimal ablation margin. Without negative margin there is no local progression, negative margins lower than 5 mm show more local tumor progression than margins in the range -5 to 0 mm.. Log-rank test shows that the curves are statistically different ($p=0.0001$)

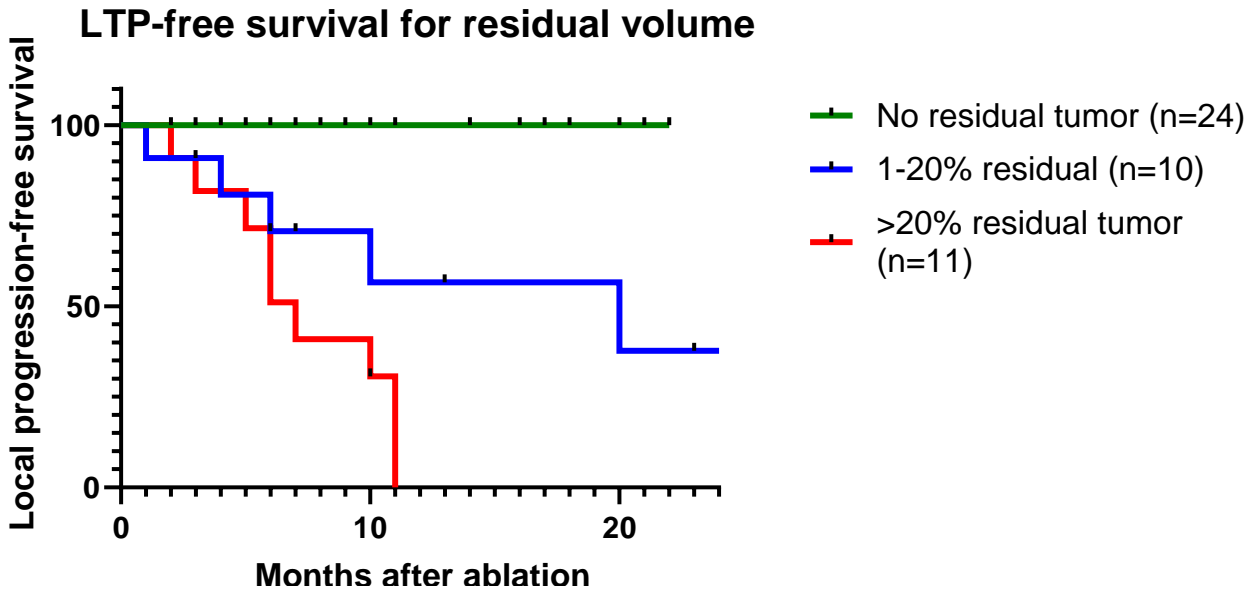


Figure 4: Kaplan-Meier curve for local progression-free survival stratified by residual tumor. When the whole tumor is covered there is no local tumor progression, the more residual tumor is left the higher the chance of local tumor progression. Log-rank test show that the curves are statistically significant ($p<0.0001$).

Discussion

Percutaneous thermal ablation is accepted as a safe and effective therapy for early stages of primary liver tumors²⁰ and second line treatment for liver metastases. However, despite progress in ablation devices, the prognosis of patients treated with thermal ablation is still impaired by LTP occurring within 2 years after ablation. In this study all percutaneous thermal ablations of liver tumors performed in the Radboudumc since 2016 were analysed. The first goal was to evaluate the 3D ablation margin of the performed ablation to test the ability to predict local tumor progression in post-ablation scans. The second goal was to determine the clinical success of MWA and RFA at our institution.

The most important finding of the 3D margin analysis was that in all cases where the tumor is fully encompassed by the ablation zone (n=24, 48% of total cases included for 3D analysis) no local tumor progression was found. When there is no residual tumor and no negative margin we see 100% local progression-free survival. All cases that show local tumor progression during follow-up are classified by the software as negative ablation margin and therefore show residual tumor volume. Therefore our data show that the software seems able to find cases that are undertreated. A number of tumors (n=5) showed negative margin (range between -5 and -9 mm) but no local tumor progression is detected, hence they are false-positive for local tumor progression. Baseline parameters do not show significant differences between cases of local tumor progression and local control. The local tumor progression rate of 28% falls well within the range of found rates in literature.⁷⁻¹⁰

Several studies performed three-dimensional measurements to provide predictions of local tumor progression after ablation. Hocquelet et al. describe a method to use the area of the tumor surface exposed to ablation margin of <5mm as a predictor for LTP using MR imaging, showing the potential of this value compared to the margin.¹⁸ Two other studies describe registration of pre-ablation CT and post-ablation CT imaging for RFA by HCC using non-rigid registration.^{21,22} Although these studies did not correlate local tumor progression with 3D ablation margins, intraprocedural use of registration software was tested. Kaye et al. performed a semi-automatic 3D assessment of the ablation zone to predict LTP, which shows volumetric assessment is feasible.¹⁷ But their study was limited by a slice thickness of 5 mm, which limits the accuracy of the assessment. In our study slices of 1 mm or 3 mm for MRI are used, which should improve the accuracy. A study of Solbiati et al. describes software for volumetric assessment after ultrasound guided MWA ablations.²³ The software uses an automatic registration algorithm (non-rigid and rigid) and shows that it can help in predicting LTP by dividing in groups of incomplete ablation and ablation plus a margin percentage. A downside is that CT imaging not performed directly after ablation and their achieved registration accuracy is not mentioned in this study.

In our study all post-ablation imaging is made immediately after the ablation, therefore this study tests the applicability of the software during the ablation procedure. Also, a relatively large group of HCC and CRLM was used which gives an insight of reached margins for both types of tumor. This heterogeneous group is also a limitation of our study as both types of tumor have different characteristics. There were also different types of ablation devices used RFA and MWA, which both have a different effect on the tissue. Both MRI and CT imaging were used for pre-ablation imaging, pre-ablation MRI makes the registration with post-ablation more difficult. These limitations all lay in the retrospective nature of this study. The follow-up time is also not equal for all tumors, therefore some tumors are not followed for 2 years yet and could still develop local progression. The registration is performed manually and is therefore time-consuming (approximate 15-30 minutes per case), which

hampers possibly use during an ablation procedure. Furthermore quantification of the exact accuracy of the registration was not performed, a small error in registration could lead to a different margin assessment. The used form of registration assessment could possibly introduce some bias in the results as it is not a quantitative assessment.

For microwave ablation several studies demonstrate tissue contraction in ex-vivo tissue especially in the central ablation zone.^{24,25,26} This makes ablation zones measured in post-treatment smaller in comparison to pre-ablation tissue. Because clinical shrinkage parameters are not yet known, the software could underestimate the size of the ablation zone measured in post-ablation scans. This could be an explanation of negative margins without the development of local tumor progression, as the area of the ablated area could be smaller on the post-ablation scan due to shrinkage. Another factor is that the software only gives the minimal distance to the ablation zone, this could give a underestimation of the ablation margin, as this could be one outlying voxel which makes it sensitive to outliers and inaccuracies in the segmentation. A 95th percentile of the minimal ablation margin could make the software less sensitive to these outliers, unfortunately the software was not able to provide this information yet. The percentage of residual tumor shows potential to be used as other prediction parameter for tumor progression. Residual tumor in combination with minimal margin could help to make the prediction less sensitive to outlying voxels.

All cases with local tumor progression have a negative ablation margin this shows that 3D volumetric assessment could help in the evaluation of the ablation zone. The software can identify ablation procedures which leave residual tumor with the chance of developing LTP. Per-procedural use of the software could help in treatment assessment and to decide whether additional ablation is necessary, although the current registration speed limits clinical use of the software. Our data suggest that 5 mm ablation margins described in literature are not necessary for adequate treatment. Most literature is based on two-dimensional assessment, which could be a reason for the difference in necessary ablation margin. As this is one of the first studies that describe three-dimensional assessment of ablation margins, further research on necessary ablation margins is advised, preferable in a prospective study with a standardized imaging and ablation protocol.

In conclusion, in our study negative ablation margins were correlated with local tumor progression following percutaneous thermal ablation of liver tumors. In our initial data, no local tumor progression was found in all cases without residual tumor. On the other hand, all tumors that showed local tumor progression also showed residual tumor. Therefore, 3D ablation assessment could help with treatment assessment and in the prediction of therapy success.

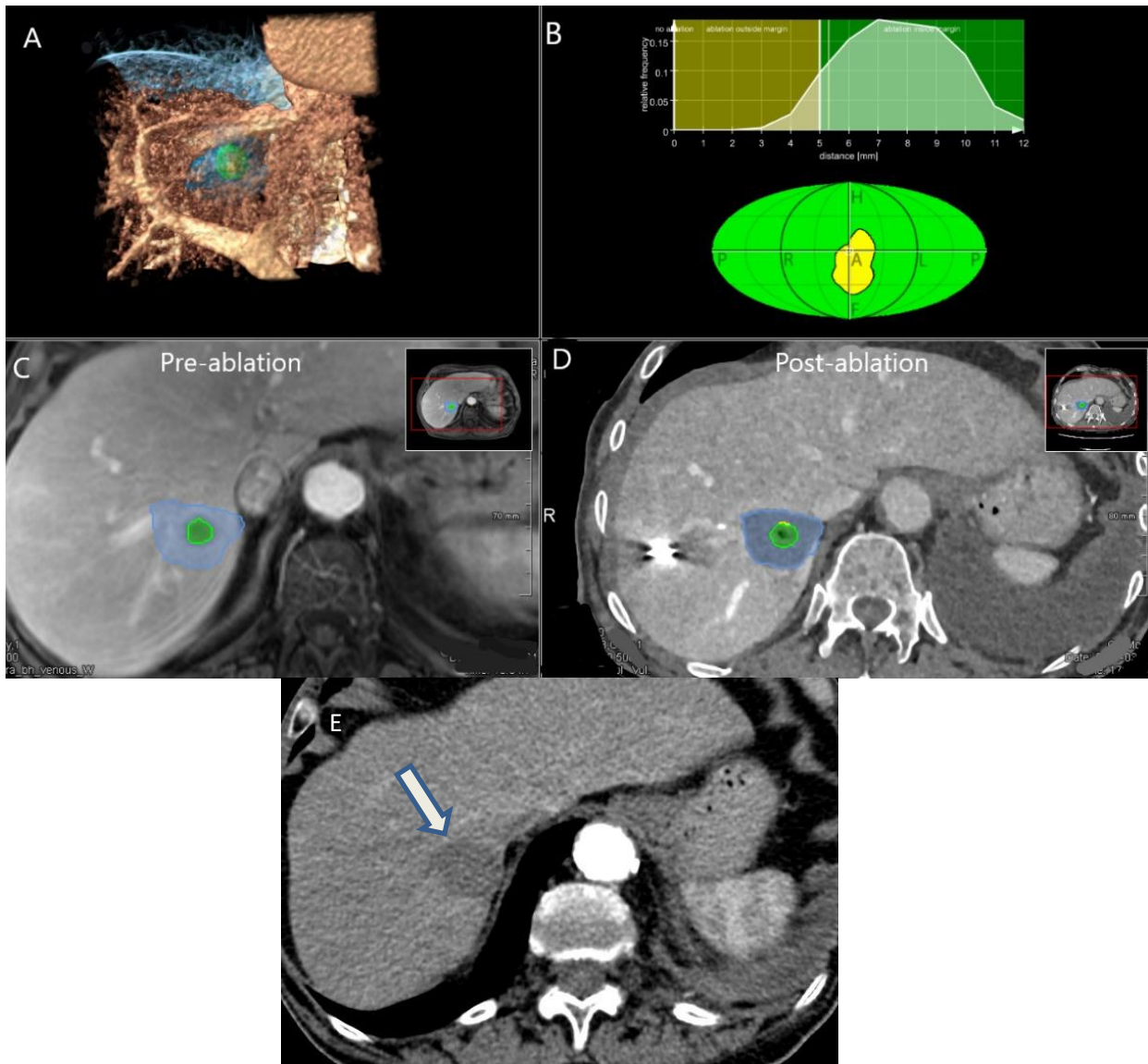


Figure 5: Representative case of local control as shown in the visualization software, in this case CRLM treated with MWA. A. 3D view of the segmented tumor and ablation zone and neighboring anatomic structures. B. Overview of margins in all directions, in green (margin > 5 mm), yellow (margin between 0-5 mm). C. Pre-ablation scan in this case MRI with in blue the segmented ablation zone and in green the segmented tumor. D. Post-ablation scan on CT (MWA applicator in situ) E: Follow-up scan after 6 months shows no signs of local tumor progression.

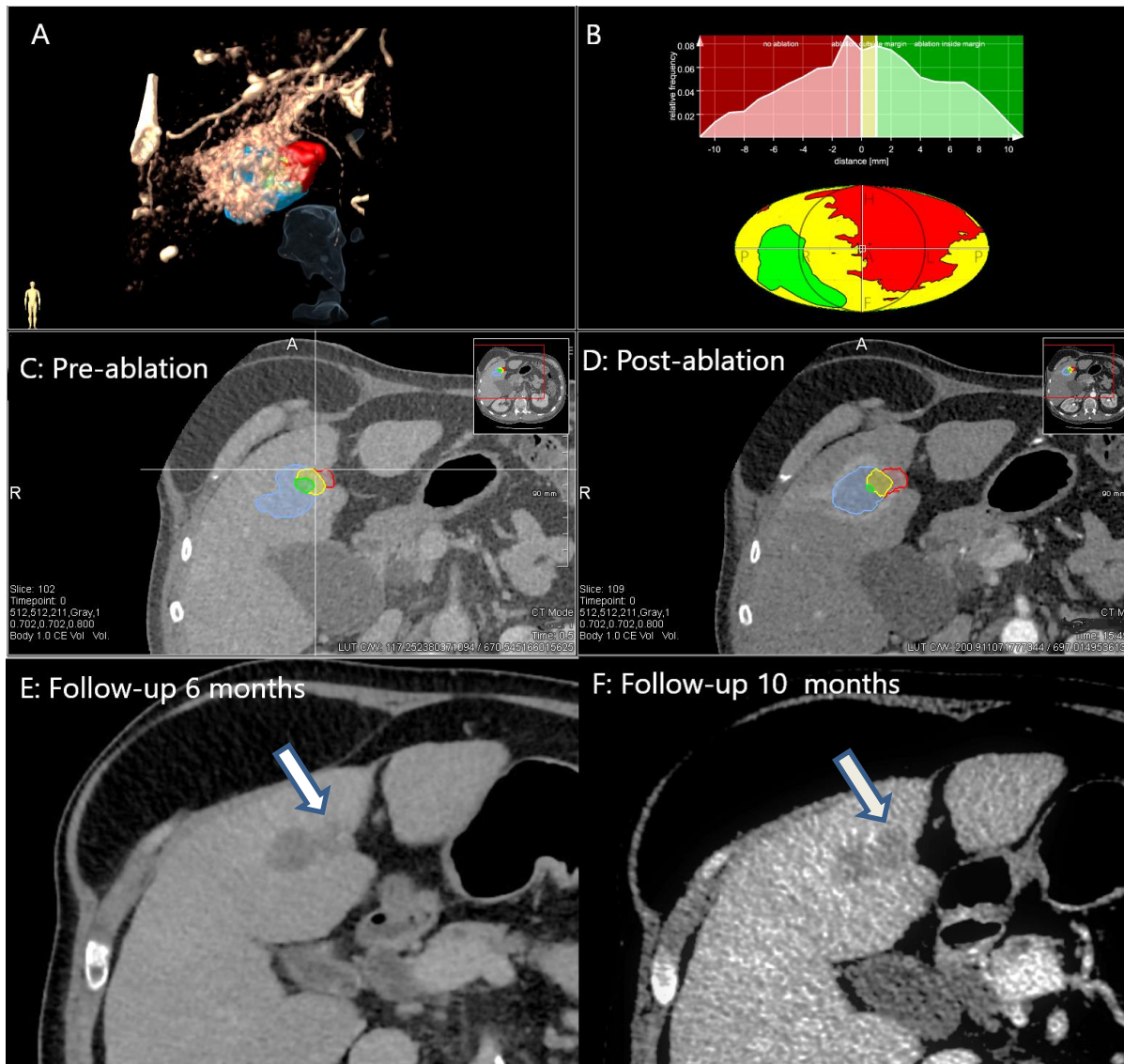


Figure 6: Example of local progression after ablation in a HCC tumor treated with MWA. 3D view of the segmented tumor and ablation zone and neighboring anatomic structures. b. Overview of margins in all directions, in green (margin > 5mm), yellow (margin between 0-5 mm) and red (margin < 0 mm, residual tumor) In the middle both pre-ablation and post-ablation imaging with the segmentations of tumor and ablation zone (green: ablation with margin, yellow: ablation with margin < 5mm and red residual tumor). Image E shows first follow-up scan performed after 6 months. Progression is visible at the same location which is marked as residual tumor (the red zone in image C and D). At F the residual tumor further progresses in size in comparison with earlier follow-up.

Chapter 3. Workflow for MR-guided liver biopsy for liver lesions in patients with pancreatic cancer

Introduction

Pancreatic cancer is one of the most lethal cancers, with a 5-year survival rate of around 5-8%.²⁷⁻²⁹ At diagnosis, approximately a third of all patients already have metastatic disease and more than half of the patients have already locally advanced pancreatic cancer. Therefore only 10-20% of the patients have a surgically resectable tumor, which is the only form of curative treatment.^{27,28,30} In case of resection a Whipple operation is performed, which consists of removal of the pancreatic head, the duodenum, the gallbladder and the distal portion of the stomach. This is a high risk procedure with a relative high risk of post-operative complications, therefore it is important to exclude liver metastases and to perform accurate staging.³¹ During exploratory surgery, approximately 17% of patients show unexpected liver metastases or locally advanced disease making the tumor unresectable. There is a large group of patients (24-53%) with tumor recurrence in the liver after surgery, of which 50% within 6 months.³² These liver metastases were probably already present during surgery, but too small to detect with routine ultrasound imaging or contrast-enhanced CT (CECT). A study performed by Danet et al. showed that in all patients with liver metastases there were lesions present with a diameter smaller than 1.5 cm, and in 81% of these patients all of the liver metastases were smaller than 1.5 cm.³³ Especially for these small lesions, diffusion-weighted MRI imaging (DWI, see appendix A for information about DWI) is superior for detection of liver lesions in comparison with CECT.³⁴ In a retrospective study of 45 patients performed at Radboudumc with diffusion-weighted and contrast-enhanced MRI, in up to 30% of patients possible liver metastases were visible, which were not visible on CECT.³⁵ To test this at a larger scale, a clinical international multi-center study (DIA-PANC study) was started to assess the diagnostic accuracy of diffusion-weighted and contrast-enhanced MRI for the detection of liver metastases in patients with pancreatic cancer. Most of the small liver lesions are not visible on trans-abdominal ultrasound, therefore it is often not possible to obtain a histopathological biopsy to prove the presence of liver metastases. Histological proof of liver metastases in patients with pancreatic cancer is important because presence of metastases excludes a curative resection of the pancreatic tumor and will change the treatment plan towards palliative therapy. In case of doubt of the suspicion of the lesion, without histological evidence, the patient will be treated with a Whipple procedure with curative intent. With the possible chance of developing liver metastases after the operation. As some liver lesions are only visible on DWI, MRI guidance could be an option to get a biopsy of these small lesions. Has the advantage of high soft tissue contrast. Another advantage of MRI is the possibility of acquiring images in arbitrary planes, this way both lesion and needle can be imaged simultaneously. A downside is the accessibility of the patient, especially in closed bore MRI. Several studies already show the possibility of MR-guided liver biopsy with good results.³⁶⁻³⁹ Therefore, the goal was to start a feasibility study (META-PANC) to determine the possibility of MRI-guided biopsies of suspicious liver lesions in patients with suspected pancreatic cancer. Before a patient study could be initiated a workflow needed to be established. Challenges include lesion visibility in combination with restraint in imaging and biopsy procedure time, respiratory motion and targeting accuracy.

There are still several uncertainties and challenges around the MR guidance of liver biopsies for pancreatic cancer which need to be solved before patient study was started. One example is the visibility of liver lesions on the different b-values was not clear. Another challenge is the effect of respiration of the patient, which moves the liver during the procedure. According to literature

respiratory motion moves the liver up to 12 mm, which could lead to missing of the target metastasis.⁴⁰ The purpose of this chapter is to describe the design of an adequate workflow for clinical application of MR-guided liver biopsy.

Materials & Methods

Materials

Several tests have been performed to improve and measure some aspects of the workflow for MR-guided liver biopsy. All experiments were performed on a 3T MRI system (Magnetom Skyra, Siemens, Erlangen, Germany). A triple modality 3D abdominal phantom (Model 057A, CIRS, Norfolk, USA) was used, as well as healthy volunteers.

Lesion re-identification

A shorter DWI scan would be useful during a biopsy procedure to reduce time for planning. The hypothesis is that a shorter DWI scan could be performed using only one b-value, the lower b-value seems most suitable as it has the highest image quality and the fastest acquisition (31 seconds).⁴¹ But the visibility of liver metastases on only b50 is not known. To make sure no lesions were missed a small retrospective study was performed on 9 patients with suspected liver metastases. For these images tumor visibility on DWI images of two b-values ($b=50 \text{ s/mm}^2$ and $b=800 \text{ s/mm}^2$), T2 HASTE and CT-images was tested by counting all suspect lesions (according the radiologist) that are visible in these scans. The DWI with $b=800$ functioned as gold truth, all marked lesions on this scan were counted in the other scans.

Coil positioning

The coil position is important for the accessibility of the puncture site is restricted, but sufficient image quality is necessary to re-identify the lesions.

The location of the coil influences both the accessibility of the liver and the image quality. To test the differences in image quality an experiment was performed with different coils types and different coil positions. For this experiment two receiver coils were used and one test in which the body coil was used as receiver. The flex coil (4 channels, dimensions: 516 mm × 224 mm) and body 18 coil (18 channels, dimensions: 385 mm × 590 mm) were placed both horizontally over the phantom and 90 degrees turned perpendicular over the phantom. This way the accessibility of the liver is better as the right side of the patient is freely accessible. All experiments were performed on the abdomen phantom using the same imaging parameters. The signal-to-noise ratio (SNR) and contrast-to-noise ratio (CNR) were calculated to test the image quality. SNR measures the level of signal compared to the background noise and the CNR is the ability to visualize different tissues through noise. Three sequences were used T2 HASTE (echo-planar fast spin echo sequence) (coronal and transversal view), DWI ($b=5$) and BEAT. Analysis was performed using RadiAnt DICOM Viewer, in this software a circular ROI was selected in the liver, the background and a tumor in the phantom.

The signal to noise ratio was calculated by: $SNR = \frac{\text{Mean signal}}{\text{std}(\text{background noise})}$

The contrast to noise ratio was determined via: $SNR \text{ liver} - SNR \text{ tumor}$

MR visible grid development

For targeting, it is important to identify the entry point of a planned needle trajectory. Because the target lesion is often not visible on real-time imaging it is important that needle is placed at exactly

the right needle path, also to avoid critical structures. To guide the interventionalist to find the right entry point a MR-grid was self-developed. Several grids have been designed and tested which is described in appendix B. This grid consist of molded silicon and is shaped as a rectangle with several grid lines which are clearly visible on MRI imaging (as shown in figure 7). The material used for the grid is EcoFlex™ 00-10 Silicone (Smooth-on Inc.) which is commercially available and safe for application to the skin. Before casting the two components of silicone were mixed, stirred and carefully poured into the mold. Any excess material was scraped off by stroking a glass bar over the surface of the mold. The grid was left to cure for at least 12 hours. Dimensions of the grid are 14,5 cm by 12 cm with a height of 3 mm. Over the length of the grid six transverse reference lines are placed within a distance of 1.5 cm from each other. Visibility of the grid was tested using the

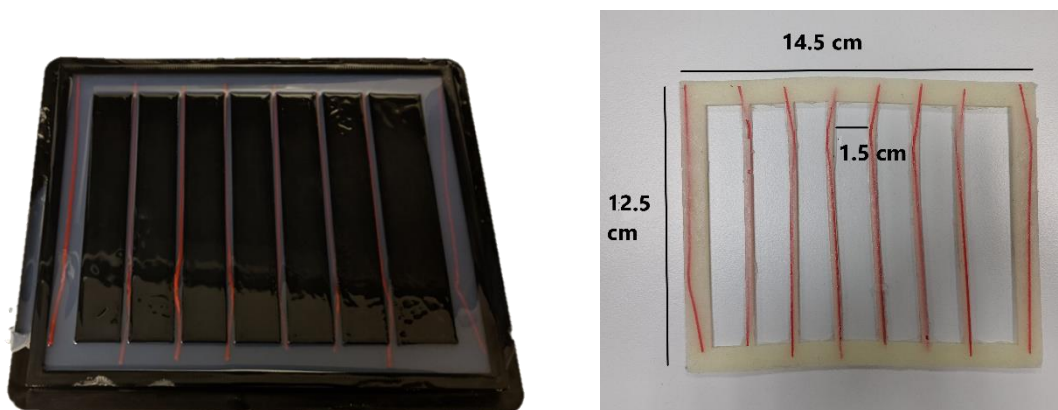


Figure 7: In this image curing of the MR-grid in the 3D printed mold is visible. After at least 12 hours the grid can be taken out of the mold and is ready for use. On the right the dimensions of the grid are visualized.

phantom.

Breathing motion

Breathing motion is a challenge during biopsy in the liver, as this moves the liver and therefore the target of biopsy. Respiratory triggering and/or comprehensive breathing instructions are therefore necessary to maintain the liver position as stable as possible. Movement of the liver during breathing was tested in a healthy test subject, to determine the variability of liver position during breathing instructions for patients. This was done by measuring the liver motion for different breathing instructions: free breathing, breath hold expiration and breath hold inspiration. Imaging was performed using the BEAT real-time sequence. The motion of the liver was measured in RadiAnt DICOM viewer by measuring the maximal motion of the liver diaphragm border in the sagittal view of the real-time BEAT sequence.

Results

Lesion re-identification

Results (visible in Table 4) show that the total visible lesions is lower for $b=50$ in comparison with $b=800$ in 4 cases out of 10 patients. Of the total lesion 44 lesions visible in DWI with $b=800$, 36 tumors are visible in the DWI with $b=50$, which means 82% is visible. But only lesions smaller than 5 mm are missed, which means for lesions bigger than 5 mm 100% of the lesions can be identified on the $b=50$

scan. Another finding is that the lesions were not visible on T2 HASTE in four patients, which might difficult the targeting as confirmation scan with the needle in the patient is not possible with DWI.

Table 4: Visibility of lesions on different scans for a small retrospective study in patients

Patient	N Lesions CT	N Lesions T2 HASTE	N Lesions DWI (b50)	N Lesions DWI (b800)
1	4	6	10	10
2	2	None	1	1
3	2	None	2	2
4	3	3	5	6
5	4	3	7	7
6	1	1	3	6
7	1	None	3	3
8	None	1	2	4
9	None	none	3	5

Coil positioning.

SNR and CNR measurements for different coil types and positions were measured that the normal horizontal placement of the body coil showed the best SNR and CNR for all four sequences. Rotated body coil performed second best in all four sequences. Table 5 shows results of the measurements for the transversal T2 HASTE sequence.

Table 5: Results of the SNR and CNR measurements for the transversal T2 HASTE sequence. The flex coil-horizontal position was expected to be better than the rotated flex coil, this was due to a difference in coil set-up for this measurement. Difference between flex coil and body coil were so pronounced no extra measurement was performed.

Coilpositions	SNR	CNR
Body RF coil	35.2	12.8
Flex coil – horizontal*	121.7	41.9
Flex coil – rotated 90°	214	44
Body coil - horizontal	290.5	105.2
Body coil – rotated 90°	266.9	58.6

MR visible grid

The MR-visible grid was tested on an abdominal phantom which shows clear visibility of the lines of the grid, therefore the grid is helpful in depicting the entry point. The final grid and a result of visibility test are shown in figure 8.

Breathing motion

The movement of the liver in free breathing was tested in two sessions a mean displacement of 8 mm was found between inspiration and expiration. The displacement between two expiration breath holds with normal breathing in between breath holds of 15 seconds, this was performed four times. With a mean motion of 1 ± 0.4 mm (range: 0.8-1.6 mm). Between two expiration breath holds the maximum difference was 1.6 mm. The maximum difference between all four measurements was 3.2 mm.

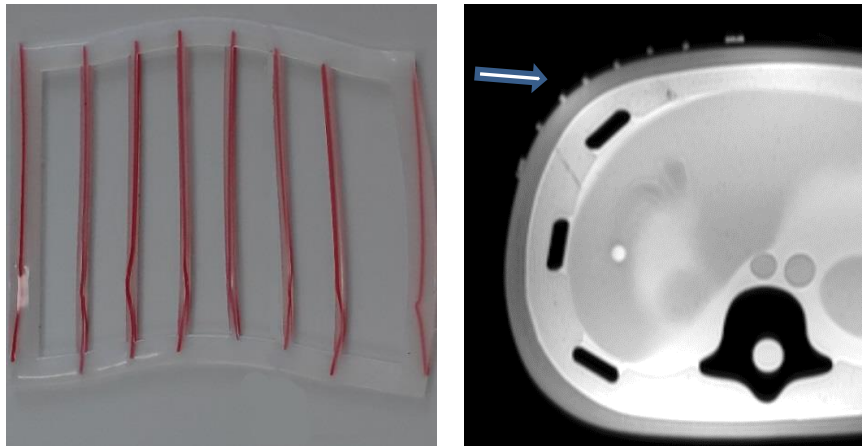


Figure 8: On the left the MR-grid, on the right a T2 HASTE image of the abdominal phantom with the MR-grid placed on top of it. The gridlines can be distinguished as hyperintense signal on top of the surface.

Imaging parameters

In clinical setting and test setting the following imaging parameters were used.

	<i>TE (ms)</i>	<i>TR (ms)</i>	<i>Flip angle</i>	<i>Slice thickness (mm)</i>	<i>FOV (mm²)</i>	<i>Acquisition time</i>
<i>T2 HASTE (transversal) (identification)</i>	87	1400	180°	5	400x400	1:19 min
<i>DWI (b50) (lesion identification)</i>	43	4000	90°	5	380x306	31 sec
<i>BEAT (targeting)</i>	2.03	383.78	30°	5.5	300x300	3 images/second
<i>T2 HASTE (biopsy confirmation)</i>	119	1100	160°	5	400x400	12 sec

Discussion

Some tests were performed to improve and gain more insight in some challenges of the workflow for MR-guided liver biopsies. The best imaging quality is reached with the body coil, the size of this coil might reduce the accessibility but the imaging quality is much better than the flex coil, therefore the body coil should be used for the biopsy. Rotation of the body coil is a possibility when the entry point is not accessible. Most lesions are visible on both b=800 and b=50, therefore a shortened DWI scan can be used during the biopsy procedure. Only when very small lesions (<5mm) are targeted a full DWI scan is necessary. The MR-grid is clearly visible on the T2 HASTE images and can therefore help in the guidance for the MR-biopsy. Expiration breath hold is the most stable breath hold position, although after a short breath the liver can shift a few millimeters. To minimize this shift extensive breath hold instructions need to be given to the patient during the procedure. The maximum time of one breath hold is 10 to 15 seconds based on the capacities of the patient.

Final targeting method

Planning imaging is not only used for visualization of the target but is also used to plan a trajectory from the skin to the target. Based on the surrounding tissue a puncture site is chosen and a needle path is planned to the target. To provide anatomical information the T2 HASTE is made in transversal and coronal direction, these scans are performed during breath-hold (expiration) to make sure the target stays on the same position. When a safe trajectory is found to reach the target lesion this trajectory is planned on the MR-console by selected an entry point and a target.

Based on the planned trajectory the MRI scanner can set the laser on exact height of the entry point using the LaserToTarget module, see figure 9. When the grid is placed on the body of the patient before scanning therefore during planning the grid lines are visible on the anatomical MR images. During planning of the trajectory the grid lines can be counted to find the position of the entry point. The grid is used in combination with the laser, the laser will give the height of the entry point, the grid provides the lateral location. The entry point can then be marked by the interventional radiologist using a MR-compatible marker. After marking this point the grid is removed and the entry site can be disinfected.

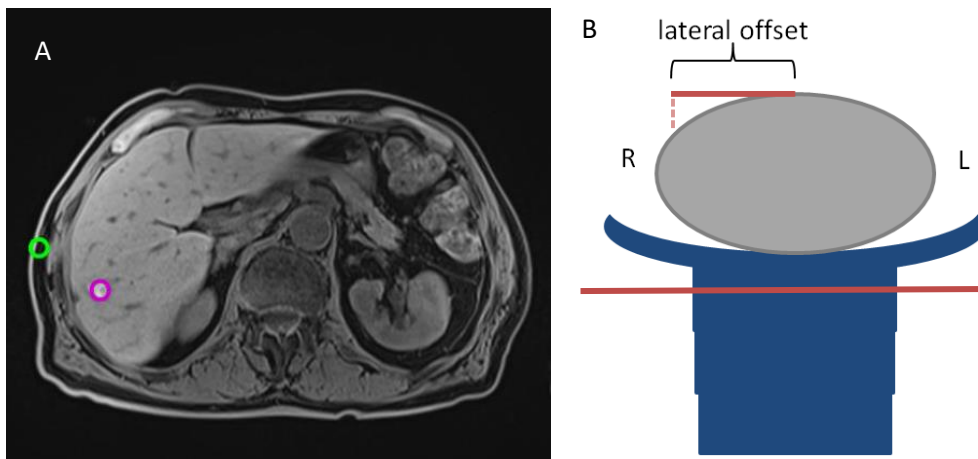


Figure 9: Still of the LaserToTarget module in green the entry point is marked, with purple the target is marked. Based on the chosen trajectory the laser is placed at the height of the entry point. For the lateral offset the MR-grid can be used, combined they provide guidance for the radiologist.

The next targeting steps involves the entrance of the needle guide, the entry point is marked on the patient. After planning of the trajectory of the needle on the MR-console, the MR-console aligns two orthogonal MR planes in axial and sagittal orientation. These planes provide the slice positions for the interactive real-time balanced steady-state free precession (BEAT) MR fluoroscopy sequence (temporal resolution of 3 images per second). This sequence is imaged on a screen inside the MR-room, the interventionalist manipulates the needle guide which is visualized in both orthogonal planes. When the needle guide is visible in both planes it means that the needle follows the planned trajectory, a third image plane provides information about the depth. When the needle guide is visible in all three planes the needle guide is placed correctly. After correct placement of the needle guide the biopsy gun can be introduced through the needle guide. This method was tested on the phantom for oblique and double oblique trajectory and was successful in hitting the target, based on the confirmation scans. An example of this test is visible in figure 9.

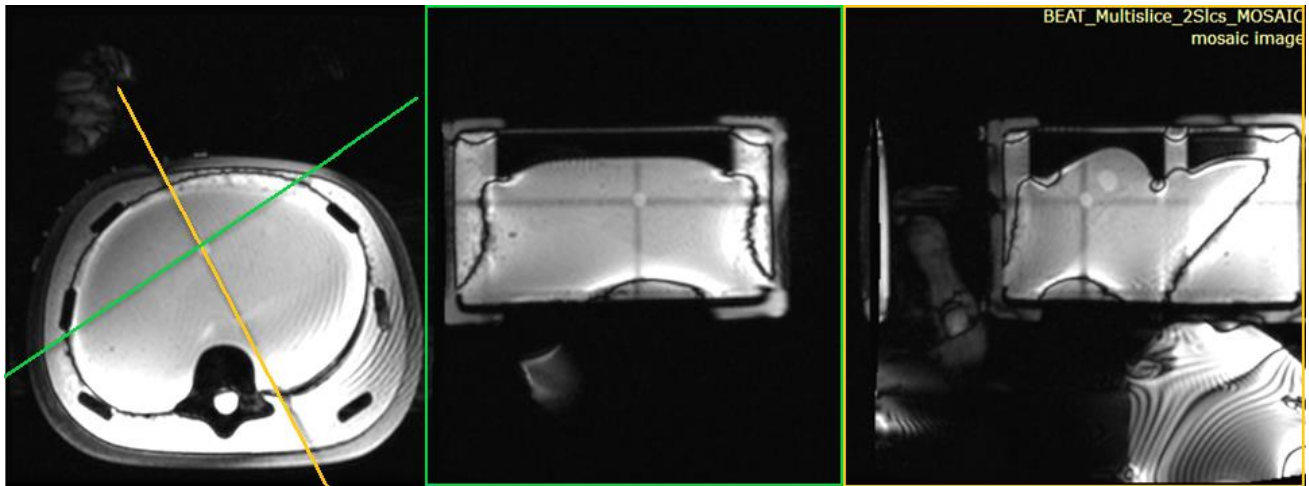


Figure 9: Example of the interactive BEAT sequence used during a test biopsy on the abdominal phantom, the image on the right and left are the orthogonal slices along the planned needle path. The colored lines show the orthogonal slices and corresponding images. Using all three slices the needle trajectory is visualized and these images help in guiding the needle towards the target.

Final workflow (flow chart shown in figure 10)

1. Patient is positioned head first supine on the MR-table
2. Localizer images are obtained to orientate the images
3. T2 HASTE images (transversal and coronal) are made for an anatomical overview and DWI are made to visualize target lesions.
4. A needle trajectory is planned on the MR-console by selecting the target and the entry point. The slices for the real-time MR sequence (BEAT-interactive multislice) are orthogonally placed based on the planned trajectory.
5. Using 'LaserToTarget' mode (for height) and the MR-grid (for lateral position), the entry point is marked on the skin of the patient.
6. The patient is disinfected and a clean working area is prepared.
7. The real-time MR sequence for visualization of the procedure is started and images are shown on the in-room screen. For every second the three images are refreshed the orientation can be checked by the radiologist by placing his finger on the marked entry point
8. A small incision is made on the entry point. The needle guide is inserted into the skin until it reaches the liver capsule.
9. The patient is instructed to exhale and to hold this breathing phase, then the needle guide can be guided towards the target based on the MR real-time images. The needle guide has to be positioned alongside the projected trajectory in both slices of the real-time MR imaging. The patient holds expiration for about 10-15 seconds, when this time ends the MR-technician announces this through the intercom which can be heard inside the MR-room.
When the needle guide is not placed near the target lesion, this step must be repeated.
10. When the needle guide is correctly placed according to the intervention team, the biopsy gun can be placed into the needle guide and towards the target lesion.
11. T2 HASTE confirmation scans in axial and sagittal direction are made to check the position of the biopsy gun and to assess if the target is hit. The biopsy can be performed when the biopsy gun is placed correctly.

12. The biopsy gun is repositioned as multiple biopsies are performed to increase the chance of a successful biopsy. After each reposition T2 HASTE images are made to assess the new position of the biopsy gun.
13. When all biopsy samples are acquired a last T2 HASTE image is made over the whole liver to check for possible complications.

Conclusion

A workflow was developed for the clinical application of MR-guided liver biopsy. Before the first patient could be included in the study the whole procedure was tested during a mock-up. In this mock-up a the workflow was used to perform a MR-guided biopsy in a phantom. After this successful mock-up the workflow was safe and complete for inclusion of the first patients.

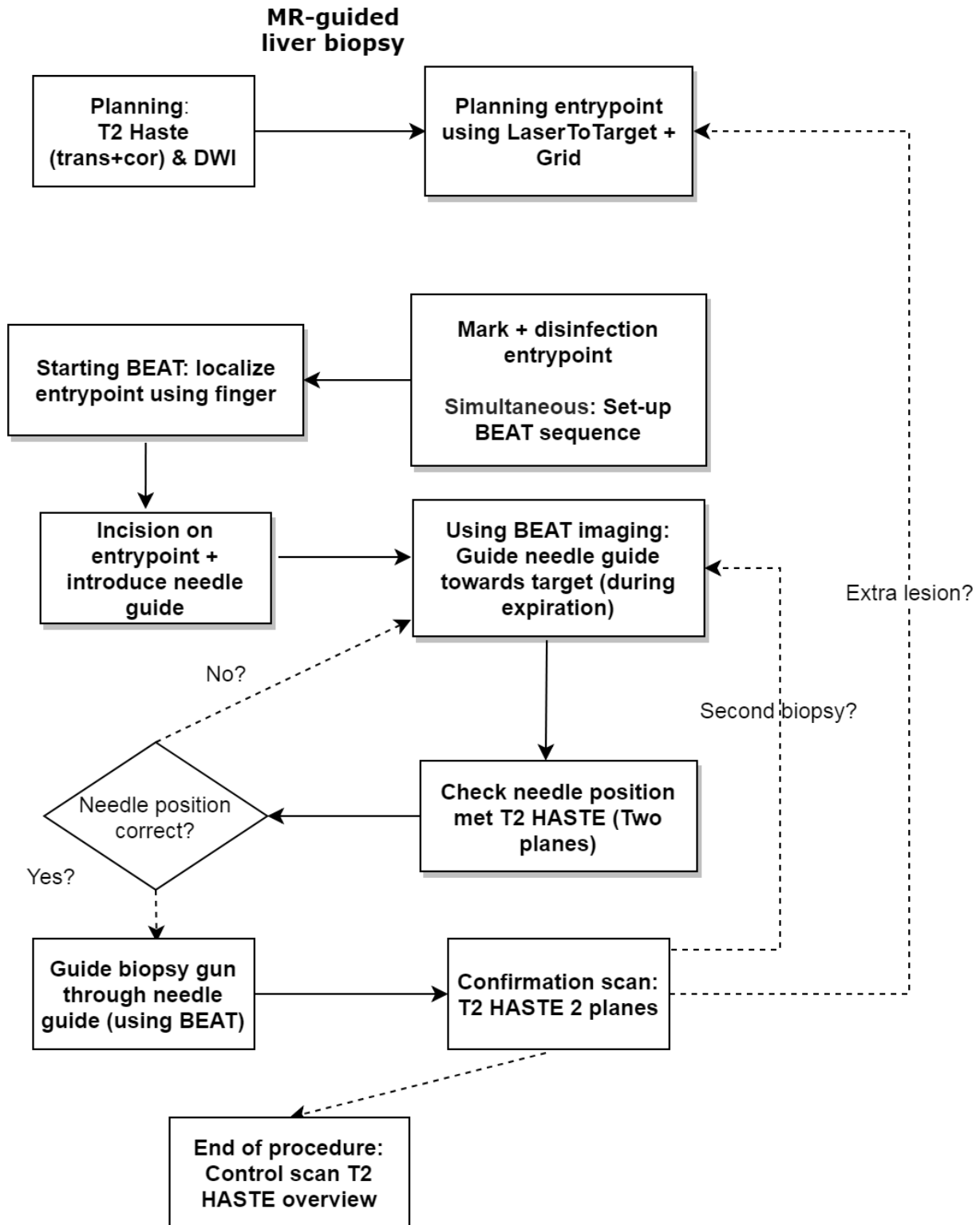


Figure 10: Flowchart of all the steps performed during the MR-guided liver biopsy procedure.

Chapter 4: META-PANC study, first clinical experience

Introduction

The META-PANC study was started because more possible liver metastases were detected using DWI, but these metastases could not be confirmed by a histopathological sample as targeted biopsy often failed. Conventional image-guidance in the form of ultrasound or CT-imaging was not sufficient, as most of these lesions are only visible on DWI. As metastases in the liver precludes curative treatment for patients with pancreatic cancer, histological proof of metastases is of utmost importance for the treatment plan of the patient. The META-PANC study will test the feasibility of MRI-guided biopsy. This study describes the first clinical experience of MR guided liver biopsies in patients with pancreatic cancer.

Materials & Methods

Biopsy procedures were performed in the Medical Innovation & Technology expert center (MITeC) using a 3.0 T closed-bore MR system (Magnetom Skyra, Siemens, Erlangen, Germany). A body 18 coil (Siemens) was used for imaging. Patients with pancreatic cancer and suspected liver lesions detected by DWI were eligible, only when an ultrasound guided biopsy was not possible. Patients had dedicated contrast-enhanced and diffusion-weighted MRI imaging performed before the MR-guided biopsy, in which suspect liver lesions were found. In both cases no lesions was visible on ultrasound and therefore no ultrasound biopsy was performed. After local anesthesia a liver biopsy is performed. Written informed consent was obtained from the subjects. To date two patients were included.

Case examples

Case 1

This is a 66-year old woman with complaints of jaundice and abdominal pain. CT imaging shows segmental narrowing of the intrapancreatic duct with a hypovascular mass in the pancreatic head. Pathology brush is suspicious for adeno carcinoma. MRI shows three lesions which are suspect for liver metastases. One is located segment 4 with high signal intensity on diffusion and contrast enhanced images. Two other lesions are located in segment 6 with high intensity on diffusion and arterial contrast enhancement. The pancreatic tumor was locally resectable, so clarity about the liver lesions was of utmost importance for the patient as confirmed metastases would preclude curative treatment. On ultrasound none of these lesions were visible and no biopsy could be performed, the patient was therefore referred for MR-guided biopsy. Before the procedure the plan was to target the lesion in segment 4 as this was marked as most suspicious for metastasis. During planning imaging the targeted lesion was not visible with T2 imaging or the DWI ($b=50$). To make sure it was not due to the adjusted imaging protocol, a full diagnostic DWI was performed (b -values ($b=50$, $b=400$, $b=800$)), but the target lesion in segment 4 could still not be found. A hyperintense lesion was found in segment 6 (see figure 11B), according to the abdominal radiologist this lesion was suspicious for metastasis and therefore it was chosen to perform biopsy of this lesion.

Using the planning software with the laser and MR-grid the entry point was marked and the needle could be guided towards the target lesion. When the coaxial needle was near the lesion, the biopsy gun was introduced and four biopsies where performed. Transversal T2 images were made to check position of the biopsy gun (as shown in figure 11D). No complications occurred during the procedure.

Final pathology shows signs no signs of metastases, extensive inflammation is present in one sample, blood and fibrotic tissue in one sample and two samples show normal liver tissue. To make sure no liver metastases were present, the patient received an additional diagnostic laparoscopy, which did not show metastases as well. As no metastases were confirmed a Whipple procedure with curative intention was performed on this patient.

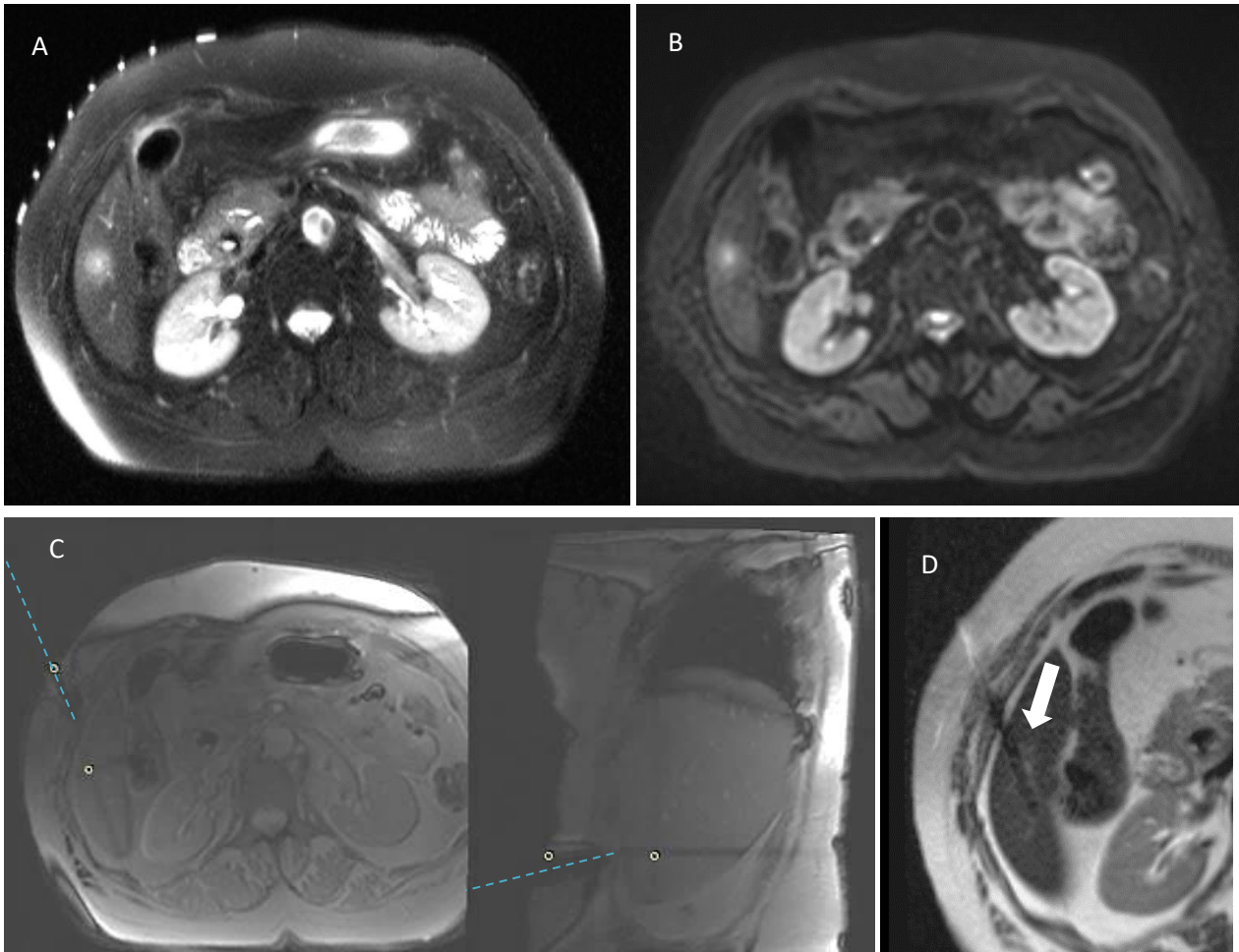


Figure 11: MRI imaging during the procedure of case 1: A shows T2-HASTE with the target lesion visible as hyperintense region in segment 6. B shows the DWI ($b=800$) of the same target lesion. C is part of the BEAT sequence, the two white rings are the planned target and entry point, the dotted line represents the needle guide. D shows the confirmation scan, a part of the target lesion is visible on the right side of the needle as pointed with the white stripe.

Case 2

This is a 68-year old woman who was diagnosed with a borderline resectable tumor in the pancreatic head with encasement of 82° of the superior mesenteric vein. The term 'borderline resectable' is used for tumors demonstrating a limited amount of arterial involvement which could eventually be resected. These patients receive neoadjuvant treatment in the form of chemotherapy or radiotherapy, after which restaging is performed to assess the possibility of complete resection again.⁴²

The needle guide was guided towards the target using the real-time MR sequence (as shown in figure 12C). The position of the needle guide was checked using the T2-HASTE in transversal and sagittal view (as shown in figure 12D). Based on these images the biopsy gun was inserted and three biopsies samples were taken. Confirmation images with the biopsy gun in situ were not possible as this did not

fit inside the bore, as the biopsy gun was bulging outside the patient due to the superficial location of the lesion. No complications occurred during the procedure. Final pathology showed no signs of metastases in the three samples, all three samples showed signs of minor periportal chronic inflammation. This patient will receive chemotherapy and undergo restaging to evaluate resectability after 3 months.

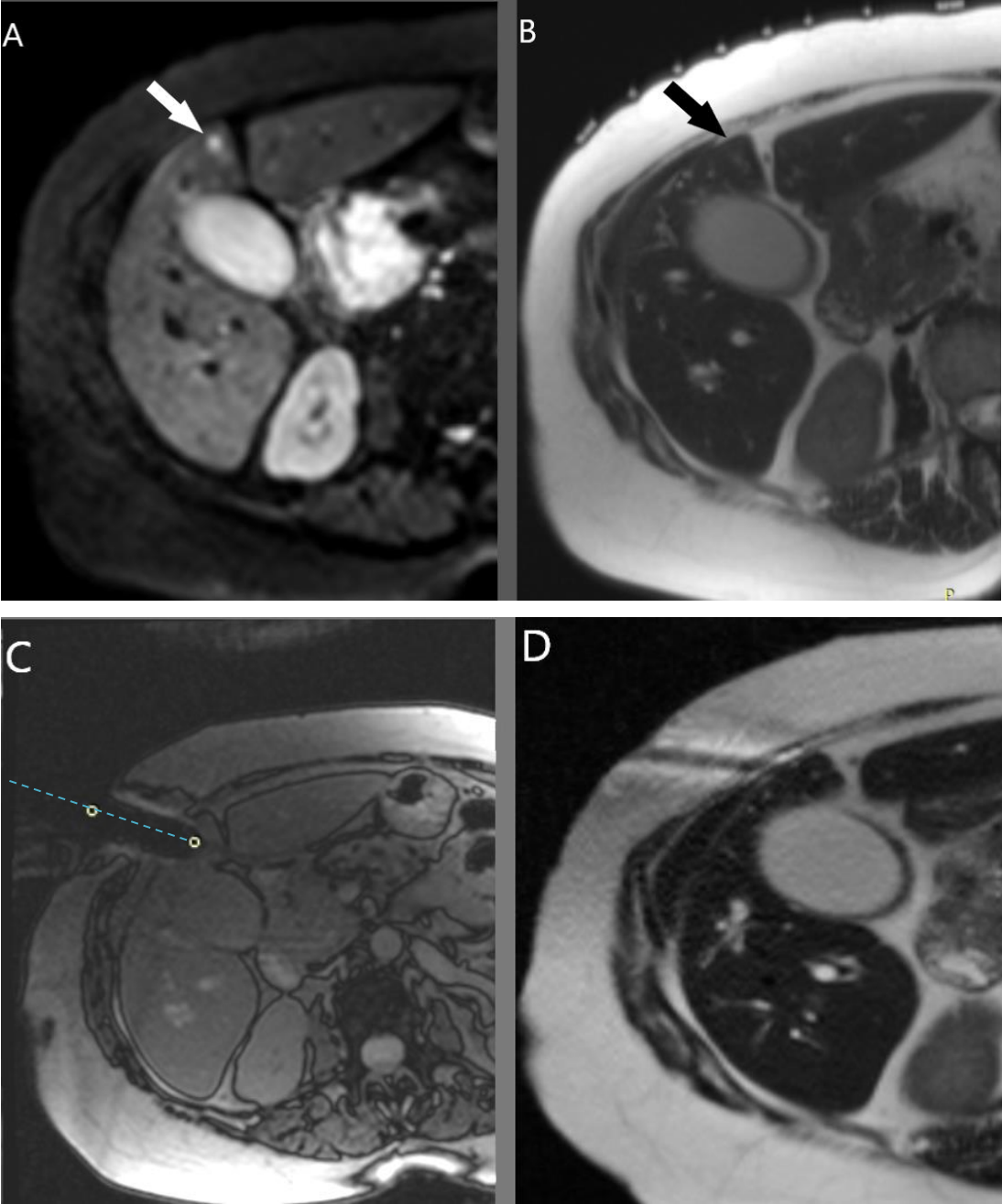


Figure 12: A: Diffusion image $b=800$, The target lesion is visible as hyperintense region. B: T2 HASTE, the target lesion is still visible, but not as pronounced as on the DWI. C: Still of the real-time BEAT sequence, the needle guide (marked with the blue dotted line) is guided towards the lesion, visible due to the large needle artefact, with the yellow circle both the entry point and target are marked. D: Confirmation scan (T2 HASTE) of the needle guide placement

Discussion

Two successful liver biopsy procedures were performed. In both cases a target lesion could be found and adequate biopsy samples were obtained. Both procedures proved that the workflow was safe and no complications occurred. However pathology did not show metastases, this may be due to a sampling error or false positive lesions on DW-MRI.

The first procedure showed the difficulty in identification of the lesions as the during diagnosis detected lesion was not visible anymore during the procedure. From the first case we also learned that DWI with only $b=50$ may not always be sufficient to detect the target lesion, to visualize the lesions a full DWI scan was performed after the short DWI (with only $b=50$). Therefore a whole DWI (with $b=50$ and $b=800$) is advised as this makes sure the lesion can be detected, although extra scan time is necessary. The second procedure was therefore performed with a diagnostic DWI instead of the shorter DWI protocol ($b=50$ only).

Not every biopsy could be checked with a confirmation scan in two directions, due to lack of procedure time or space in the bore. As the target lesions are not visible on the real-time imaging, the targeting is completely based on the planning imaging, a small change in liver location due to breathing could lead to missing the target. Due to the bore size confirmation imaging is not always possible with the biopsy gun in situ, as for superficial targets the biopsy gun sticks out. For these cases confirmation scans could only be made with the needle guide in place, small movement between the time of scanning and the time of the biopsy could displace the needle guide and therefore lead to missing the target.

The biggest challenge remains the breathing of the patient, despite comprehensive breathing instructions it remains difficult to maintain the same expiration height and therefore the liver might shift. A small shift in liver position could lead to missing the target especially when the target is not visible during targeting, which is the case for this patient group.

Another possibility was that target lesion of the biopsy was not a metastasis and therefore diagnostic imaging is not able to distinguish liver metastases well enough. The diagnosis of these liver lesions is still under research in the DIA-PANC study, therefore the exact sensitivity of DWI is not well known yet. All patients included in this study will be monitored using DWI-MRI and CECT, over time this will give more information about the nature of the targeted lesions.

The first clinical experience showed that MR-guided biopsy was feasible and safe in two patients. More patients and follow-up is required to determine the value in the staging of patients with pancreatic cancer.

Chapter 5: Conclusions & Future perspective

In this thesis two projects in image-guided liver interventions were conducted. This chapter provides the general outcomes of the thesis, based on the research questions and sub questions as mentioned in chapter one.

In chapter two a retrospective analysis on liver ablations was described. Of the total group of tumors (n=74), local tumor progression was shown in 21 tumors giving a local progression rate of 28%. In literature, local tumor progression rates in the range 8-32% are reported.

Three-dimensional analysis of treatment assessment using registration of pre- and post-ablation with segmentation of the tumor and ablation zone was possible in 45/74 (61%) cases. The other cases were excluded for ablation margin assessment due to inadequate registration or segmentation. In cases where accurate registration and visualization were possible, the software is helpful and able to give a prediction about ablation adequacy.

A correlation was found between minimal ablation margins and clinical outcome of the patient. In the group with local tumor progression, all minimal margins were negative and the minimal margin was significantly smaller ($p=0.05$) compared to the margin of the group without local tumor progression. To assess the effect on local progression-free survival a Kaplan-Meier analysis was performed: this showed a clear difference between groups divided by minimal ablation margin. For patients without negative margins a 1-year LTP-free survival of 100% was found, the group with margins of (-5-0) and the group of (<-5 mm) showed a 1-year LTP-free survival of 65% and 0%, respectively.

As all tumors with local progression had negative margins, our data shows that full encompassment of the tumor by the ablation zone is enough to prevent local tumor recurrence and no extra ablation margin is necessary.

In chapter three some challenges in the workflow for MR-guided liver biopsy were described, which include motion due to breathing, positioning of coil, fast identification of the entry point during the procedure. Breathing instructions were used to reduce the liver motion as much as possible, although this remains a possible problem during the procedure. Image quality using different coil setups was tested, the body coil showed the best imaging quality and should be used when possible. An MR-grid can help in identifying the entry point in a fast and practical manner. With these improvements an adequate workflow for clinical application was developed and tested.

In chapter four the first clinical experience with the MRI-guided biopsy was described. The MR-guided biopsy was feasible and safe in two patients. The first two procedures were performed safe as no procedure complications did arise during these procedures. This means the technique is safe enough to be implemented. Although clear patient instructions are necessary to perform the procedure in a safe and accurate manner, as the liver motion is of big influence on the procedure. More patients and follow-up are required to determine the value in the staging of patients with pancreatic cancer.

Future Perspectives

In this retrospective study 3D ablation margins show a correlation with local treatment progression after ablation. Therefore 3D ablation margins could help in the treatment assessment during and after an ablation procedure. This software is almost ready for use in clinical practice, although the necessary time for registration is often too long. Accurate 3D registration and segmentation are not always

possible due to misalignments between pre- and post-ablation images. Although the software does show potential to help in improving treatment assessment during ablation procedures.

To test the potential of treatment assessment during ablation further research is advised, this could be implemented in a prospective study with standardized imaging and ablation protocol. Pre- and post-ablation imaging in the same patient position with the same breathing phase (in apnea), would make registration of these images simpler and more accurate. By using the software during ablation procedures, the hypothesis is that residual tumor can be found in an earlier state and the tumor could be re-ablated during the same procedure.

A way to prove the additional value of 3D visualization during the procedure would be a comparison of ablation procedures performed with conventional 2D treatment assessment and ablations performed with 3D ablation treatment assessment. After correlating these outcomes with local tumor progression after a follow-up period, the best way of treatment assessment can be found, hopefully reducing the rate of local tumor progression.

To improve patient selection for ablation procedures predicting factors for local tumor progression would be useful. During this retrospective study no predicting baseline parameters were found, but not all ablation data is analyzed yet, such as applied ablation time and ablation energy. Further analysis of this data might give more prediction parameters for local tumor progression.

In this thesis the workflow for MR-guided liver biopsy was tested for MRI-guided liver biopsy. The clinical study in patients with pancreatic cancer will continue to determine the value of this technique for the staging of these patients. The developed workflow could also be used for other purposes, as the image guidance of a biopsy needle is the same as for an ablation applicator the workflow for liver biopsies could also be applied for MR-guided liver ablation. MRI-guidance for ablations shows possible advantages compared to conventional CT or ultrasound guidance, such as higher sensitivity in depicting small lesions, multiplanar imaging and the possibility of monitoring thermal effects during ablation. To test this a study will start in the Radboudumc with the use of MR-guidance during thermal ablation of liver tumors. The goal of this study is to assess the feasibility of real-time MRI temperature monitoring and ablation zone assessment during thermal ablation in the liver. Therefore the MR-guided liver biopsy could be a first step towards other MR-guided liver interventions.

In summary, this thesis presented two projects to improve image guidance for liver interventions. 3D treatment assessment is useful for prediction ablation outcome because all tumors with local tumor progression show a negative ablation margin. A MR-guided liver biopsy workflow was developed and proved feasible. Both techniques could help to improve image guidance of liver interventions in future clinical practice.

References

1. Solomon SB, Silverman SG. Imaging in Interventional Oncology. *Radiology*. 2010;257(3):624-640. doi:10.1148/radiol.10081490
2. van Amerongen M, Jenniskens S, van den Boezem P, Fütterer J, de Wilt J. Radiofrequency ablation compared to surgical resection for curative treatment of patients with colorectal liver metastases – a meta-analysis. *Hpb*. 2017;19(9):749-756. doi:10.1016/j.hpb.2017.05.011
3. Kao W, Chiou Y, Hung H, et al. Risk factors for long-term prognosis in hepatocellular carcinoma after radiofrequency ablation therapy : the clinical implication of aspartate aminotransferase – platelet ratio index. 2011:1-9. doi:10.1097/MEG.0b013e328346d529
4. Goldberg S, Gazelle G, Mueller P. Thermal Ablation Therapy for Focal Malignancy : A Unified Approach to Underlying Principles, Techniques, and Diagnostic Imaging Guidance. *Eur J Ultrasound*. 2000;(February):323-331.
5. Livraghi T, Solbiati L, Meloni F, Ierace T, Goldberg SN, Gazelle GS. Percutaneous radiofrequency ablation of liver metastases in potential candidates for resection: The “test-of-time” approach. *Cancer*. 2003;97(12):3027-3035. doi:10.1002/cncr.11426
6. Galle P, Forner A, Llovet JM, et al. Clinical Practice Guidelines Of Hepatology EASL Clinical Practice Guidelines : Management of hepatocellular carcinoma. *J Hepatol*. 2018;69(1):182-236. doi:10.1016/j.jhep.2018.03.019
7. Napoleone M, Kielar AZ, Hibbert R, Saif S, Kwan BYM. Local tumor progression patterns after radiofrequency ablation of colorectal cancer liver metastases. *Diagnostic Interv Radiol*. 2016;22(6):548-554. doi:10.5152/dir.2016.15543
8. Tanis E, Nordlinger B, Mauer M, Sorbye H, Coevorden F Van. Local recurrence rates after radiofrequency ablation or resection of colorectal liver metastases . Analysis of the European Organisation for Research and Treatment of Cancer # 40004 and # 40983 q. *Eur J Cancer*. 2014;50(5):912-919. doi:10.1016/j.ejca.2013.12.008
9. Yu J, Liang P, Yu X, Cheng Z. Local tumour progression after ultrasound-guided microwave ablation of liver malignancies : risk factors analysis of 2529 tumours. 2015:1119-1126. doi:10.1007/s00330-014-3483-4
10. Lam V, Ng K, Hk M, et al. Incomplete Ablation After Radiofrequency Ablation of Hepatocellular Carcinoma : Analysis of Risk Factors and Prognostic Factors. 2007;15(3):782-790. doi:10.1245/s10434-007-9733-9
11. Liu C, Yu C, Chang W, Dai M, Hsiao C, Chou Y. Radiofrequency ablation of hepatic metastases: Factors influencing local tumor progression. *Ann Surg Oncol*. 2014;21(9):3090-3095. doi:10.1245/s10434-014-3738-y
12. Shady W, Petre EN, Gonen M, et al. Percutaneous Radiofrequency Ablation of Colorectal Cancer Liver Metastases: Factors Affecting Outcomes—A 10-year Experience at a Single Center. *Radiology*. 2016;278(2):601-611. doi:10.1148/radiol.2015142489
13. Kim Y, Lee W, Rhim H, Lim H, Choi D, Lee J. The minimal ablative margin of radiofrequency ablation of hepatocellular carcinoma (> 2 and < 5 cm) needed to prevent local tumor progression: 3D quantitative assessment using CT image fusion. *Am J Roentgenol*. 2010;195(3):758-765. doi:10.2214/AJR.09.2954

14. Sasaki A, Kai S, Iwashita Y, Hirano S, Ohta M, Kitano S. Microsatellite distribution and indication for locoregional therapy in small hepatocellular carcinoma. *Cancer*. 2005;103(2):299-306. doi:10.1002/cncr.20798
15. Nakazawa T, Kokubu S, Shibuya A, et al. Radiofrequency ablation of hepatocellular carcinoma: Correlation between local tumor progression after ablation and ablative margin. *Am J Roentgenol*. 2007;188(2):480-488. doi:10.2214/AJR.05.2079
16. Wang X, Sofocleous CT, Erinjeri JP, Solomon SB. Margin Size is an Independent Predictor of Local Tumor Progression After Ablation of Colon Cancer Liver Metastases. 2013:166-175. doi:10.1007/s00270-012-0377-1
17. Kaye E, Cornelis F, Petre E, et al. Volumetric 3D assessment of ablation zones after thermal ablation of colorectal liver metastases to improve prediction of local tumor progression. *European Radiology*. 2018.
18. Hocquelet A, Trillaud H, Frulio N, et al. Three-Dimensional Measurement of Hepatocellular Carcinoma Ablation Zones and Margins for Predicting Local Tumor Progression. *J Vasc Interv Radiol*. 2016;27(7):1038-1045.e2. doi:10.1016/j.jvir.2016.02.031
19. Teng W, Liu KW, Lin CC, et al. Insufficient ablative margin determined by early computed tomography may predict the recurrence of hepatocellular carcinoma after radiofrequency ablation. *Liver Cancer*. 2015;4(1):26-38. doi:10.1159/000343877
20. Galle P, Forner A, Llovet J, et al. EASL Clinical Practice Guidelines: Management of hepatocellular carcinoma. *J Hepatol*. 2018. doi:10.1016/j.jhep.2018.03.019
21. Kim K, Lee J, Klotz E, et al. Safety margin assessment after radiofrequency ablation of the liver using registration of preprocedure and postprocedure CT images. *Am J Roentgenol*. 2011;196(5):565-572. doi:10.2214/AJR.10.5122
22. Shin S, Lee J, Kim KW, et al. Postablation assessment using follow-up registration of CT images before and after radiofrequency ablation (RFA): Prospective evaluation of midterm therapeutic results of RFA for hepatocellular carcinoma. *Am J Roentgenol*. 2014;203(1):70-77. doi:10.2214/AJR.13.11709
23. Solbiati M, Muglia R, Goldberg SN, et al. A novel software platform for volumetric assessment of ablation completeness. *Int J Hyperth*. 2019;36(1):337-343. doi:10.1080/02656736.2019.1569267
24. Farina L, Weiss N, Nissenbaum Y, et al. Characterisation of tissue shrinkage during microwave thermal ablation. *Int J Hyperth*. 2014;30(7):419-428. doi:10.3109/02656736.2014.957250
25. Amabile C, Farina L, Lopresto V, et al. Tissue shrinkage in microwave ablation of liver: an ex vivo predictive model. *Int J Hyperth*. 2017;33(1):101-109. doi:10.1080/02656736.2016.1208292
26. Liu D, Brace CL. CT imaging during microwave ablation: Analysis of spatial and temporal tissue contraction. *Med Phys*. 2014;41(11):1-9. doi:10.1118/1.4897381
27. American Cancer Society. Cancer Facts & Figures. *Cancer*. 2017. doi:10.1097/01.NNR.0000289503.22414.79
28. Ilic M, Ilic I. Epidemiology of pancreatic cancer. *World J Gastroenterol*. 2016;22(44):9694-9705. doi:10.3748/wjg.v22.i44.9694

29. Dutch Pancreatic Cancer Group. Nieuwe ontwikkelingen in de behandeling van het pancreascarcinoom. *Ned Tijdschr Geneeskd.* 2016;160:1-7.
30. Balaban E, Mangu P, Khorana A, et al. Locally advanced, unresectable pancreatic cancer: American society of clinical oncology clinical practice guideline. *J Clin Oncol.* 2016;34(22):2654-2667. doi:10.1200/JCO.2016.67.5561
31. Warshaw A, Lillemoe K, Fernandez-Del Castillo C. Pancreatic surgery for adenocarcinoma. *Curr Opin Gastroenterol.* 2012;28(5):488-493. doi:10.1097/MOG.0b013e3283567f2c
32. Van den Broeck A, Sergeant G, Ectors N, Van Steenberghe W, Aerts R, Topal B. Patterns of recurrence after curative resection of pancreatic ductal adenocarcinoma. *Eur J Surg Oncol.* 2009;35(6):600-604. doi:10.1016/j.ejso.2008.12.006
33. Danet I, Semelka R, Nagase L, Woosely J, Leonardou P, Armao D. Liver metastases from pancreatic adenocarcinoma: MR imaging characteristics. *J Magn Reson Imaging.* 2003;18(2):181-188. doi:10.1002/jmri.10337
34. Holzapfel K, Reiser-Erkan C, Fingerle AA, et al. Comparison of diffusion-weighted MR imaging and multidetector-row CT in the detection of liver metastases in patients operated for pancreatic cancer. *Abdom Imaging.* 2011;36(2):179-184. doi:10.1007/s00261-010-9633-5
35. Hermans J, Riviere D, van Geenen E, Radema S, Nagtegaal I, van Laarhoven K. Contrast-enhanced diffusion-weighted MRI versus contrast-enhanced CT for detecting liver metastases for potentially resectable pancreatic ductal adenocarcinoma. *Pancreatology.* 2016;16(3):S68. doi:10.1016/j.pan.2016.05.231
36. Fischbach F, Bunke J, Thormann M, et al. MR-guided freehand biopsy of liver lesions with fast continuous imaging using a 1.0-T open MRI scanner: Experience in 50 patients. *Cardiovasc Intervent Radiol.* 2011;34(1):188-192. doi:10.1007/s00270-010-9836-8
37. Smith E, Grove J, Van Der Spek A, Jarboe MD. Magnetic-resonance-guided biopsy of focal liver lesions. *Pediatr Radiol.* 2017;47(6):750-754. doi:10.1007/s00247-017-3788-y
38. Moche M, Heinig S, Garnov N, et al. Navigated MRI-guided liver biopsies in a closed-bore scanner: experience in 52 patients. *Eur Radiol.* 2016;26(8):2462-2470. doi:10.1007/s00330-015-4097-1
39. Das C, Goenka A, Srivastava D. MR-guided abdominal biopsy using a 1.5-Tesla closed system: A feasibility study. *Abdom Imaging.* 2010;35(2):218-223. doi:10.1007/s00261-009-9504-0
40. Ruitian S, Tipirneni A, Johnson P. Evaluation of respiratory liver and kidney movements for MRI navigator gating. *J Magn Reson Imaging.* 2011;70(12):773-779. doi:10.1097/OGX.0000000000000256.Prenatal
41. Goshima S, Kanematsu M, Kondo H, et al. Diffusion-weighted imaging of the liver: Optimizing b value for the detection and characterization of benign and malignant hepatic lesions. *J Magn Reson Imaging.* 2008;28(3):691-697. doi:10.1002/jmri.21467
42. Lopez N, Prendergast C, Lowy A. Borderline resectable pancreatic cancer: Definitions and management. *World J Gastroenterol.* 2014;20(31):10740-10751. doi:10.3748/wjg.v20.i31.10740
43. Taouli B, Koh D. Diffusion-weighted MR imaging of the liver. *Radiology.* 2010;254(1):47-66. doi:10.1148/radiol.09090021

44. Bharwani N, Koh D. Diffusion-weighted imaging of the liver: an update. *Cancer Imaging*. 2013;13(2):171-185. doi:10.1102/1470-7330.2013.0019
45. Park M, Kim Y, Choi S-Y, Rhim H, Lee WJ, Choi D. Preoperative Detection of Small Pancreatic Adenocarcinoma: Value of Adding Diffusion-weighted Imaging to Conventional MR Imaging for Improving Confidence Level. *Radiology*. 2014;273(2):132563. doi:10.1148/radiol.14132563

Appendix A: Diffusion-weighted imaging

DWI is a functional imaging technique which derives image contrast on the basis of differences in diffusivity of water molecules within tissues. In high cellular tissue (such as tumor tissue) diffusion is restricted, in necrotic or cystic tissue the diffusion is relatively free. The basis diffusion weighted sequence is a modified T2-weighted imaging sequence, with a symmetric pair of diffusion-sensitizing gradients on both sides of the 180° refocusing pulse. Water protons acquire a phase shift from the first diffusion-sensitizing gradient, when these protons move after the first gradient the protons are not entirely re-phased in the second gradient which results in attenuation of the signal. Therefore the presence of diffusion is observed as a loss of signal and restricted diffusion shows a higher signal.^{43,44}

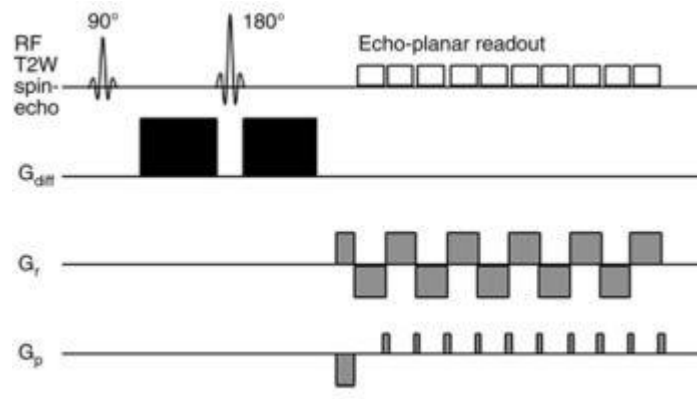


Figure 13: Gradient acquisition scheme of a basic DWI sequence. The diffusion gradients are placed on either side of the 180° refocusing pulse. The echo-planar readout results in a faster acquisition.

DWI seems to have added value for the detection of sub-centimeter liver lesions, which are often present in patients with pancreatic cancer.^{34,45} The diffusion weighing can be adjusted using varying b-values, for a higher b-value a stronger and longer diffusion gradient is used, which will result in a higher degree of diffusion weighting. A cyst has a relative lower restriction than a metastasis and shows high signal on a lower diffusion gradient ($b=50 \text{ s/mm}^2$) but shows low signal on high a diffusion gradient ($b=800 \text{ s/mm}^2$), a metastasis remains visible on a higher diffusion gradient. Therefore different b-values help to distinguish between liver lesions. Different b-values are necessary for diagnosis, but a disadvantage of multiple b-values is the relative high acquisition time. To speed up the acquisition echo-planar imaging is used, this means an entire image is acquired in a single excitation which is done by rapidly switching the read-out gradient in the frequency direction. For diagnostic imaging of liver metastases a single shot echo-planar spin echo sequence is used with three different b-values ($b=50, 400, 800 \text{ s/mm}^2$).